VOLUME 111, NUMBER 13
JUNE 21, 1989


JOURNAL OF THE AMERICAN CHEMICAL SOCIETY

# Mechanistic Study of Oscillations and Bistability in the Cu(II)-Catalyzed Reaction between $H_2O_2$ and KSCN[1]

**Yin Luo,[†] Miklós Orbán,[‡] Kenneth Kustin,[†] and Irving R. Epstein*,[†]**

*Contribution from the Department of Chemistry, Brandeis University, Waltham, Massachusetts 02254, and Institute of Inorganic and Analytical Chemistry, L. Eötvös University, H-1443, Budapest, Hungary.* *Received January 3, 1989*

**Abstract:** The $CuSO_4$-catalyzed reaction of hydrogen peroxide with thiocyanate ion is the first example of a homogeneous, liquid phase, halogen-free system that oscillates under batch conditions. A detailed mechanism is proposed consisting of 30 reactions and 26 variables. The mechanism is constructed from two nonautocatalytic mechanisms for the subsystems alkaline $H_2O_2$–$CuSO_4$ and $H_2O_2$–KSCN, coupled through various intermediates to construct a feedback network, which leads to oscillatory behavior in both batch and flow configurations. The integrated mechanism simulates very well the experimentally observed oscillations in absorbance and $O_2$ evolution and two of the three kinds of bistability in a continuously stirred tank reactor. Two alternative mechanisms are also considered, providing insight into the general properties of oscillatory mechanisms.

Since the systematic design of homogeneous liquid-phase chemical oscillators began[2] a decade ago, reaction families based on oxyhalogen species have dominated the field. The advantage of using halogen or oxyhalogen species in constructing chemical oscillators lies in their fast reaction rates and multiple oxidation states. Only recently has progress been made in finding halogen-free chemical oscillators, providing further evidence of the generality of nonmonotonic behavior, which had long been denied or ignored by many chemists. Although they are fewer in number than the halogen-based systems, the known halogen-free (or non-halogen-based) chemical oscillators already show a wide range of behavior, opening up further opportunities for systematic design. Important examples include the oxidation of benzaldehyde by oxygen in glacial acetic acid with a $CoBr_2$ catalyst,[3] the oxidation of methylene blue by oxygen in strongly alkaline medium in the presence of sulfite and sulfide,[4] and two permanganate-reductant oscillators.[5] A group of oscillators discovered by Orbán and Epstein involves the hydrogen peroxide oxidation of sulfide,[6] thiosulfate,[7] (catalyzed by $CuSO_4$) and thiocyanate[8] (catalyzed by $CuSO_4$). Despite the apparent similarity of their constituents, these systems are mechanistically quite different. The $H_2O_2$–KSCN–$CuSO_4$ system oscillates only above pH 9, and its pH is essentially constant during the oscillation in color and Pt potential.[8] The other two systems, in contrast, are driven by pH changes of several units.[6,7] Another special feature of the $H_2O_2$–KSCN–$CuSO_4$ system is the slowly damped oscillation under batch conditions. Such batch oscillations are quite rare, even among the much larger group of halogen-based chemical oscillators.

Mechanisms for oscillatory chemical systems have been pursued almost as soon as chemists finally recognized the possibility of oscillation in a homogeneous medium. Understanding why and how such complicated behavior arises in terms of chemical species and the interactions among them is a fascinating subject in itself. In addition, this understanding facilitates the further design of new chemical oscillators. A successful mechanistic study also contributes to knowledge of the general chemistry and kinetics of the chemical species that are involved. A good example is the

[†] Brandeis University.
[‡] L. Eötvös University.

(1) Part 51 in the series Systematic Design of Chemical Oscillators. Part 50: Rábai, Gy.; Beck, M. T.; Kustin, K.; Epstein, I. R. *J. Phys. Chem.* **1989**, *93*, 2853.
(2) De Kepper, P.; Epstein, I. R.; Kustin, K. *J. Am. Chem. Soc.* **1981**, *103*, 2133.
(3) Jensen, J. H. *J. Am. Chem. Soc.* **1983**, *105*, 2639.
(4) Burger, M.; Field, R. J. *Nature (London)* **1984**, *307*, 720.
(5) (a) Nagy, A.; Treindl, L. *Nature (London)* **1986**, *320*, 344. (b) Treindl, L.; Nagy, A. *Chem. Phys. Lett.* **1987**, *138*, 327.
(6) Orbán, M.; Epstein, I. R. *J. Am. Chem. Soc.* **1985**, *107*, 2302.
(7) Orbán, M.; Epstein, I. R. *J. Am. Chem. Soc.* **1987**, *109*, 101.
(8) Orbán, M. *J. Am. Chem. Soc.* **1986**, *108*, 6893.

0002-7863/89/1511-4541$01.50/0 

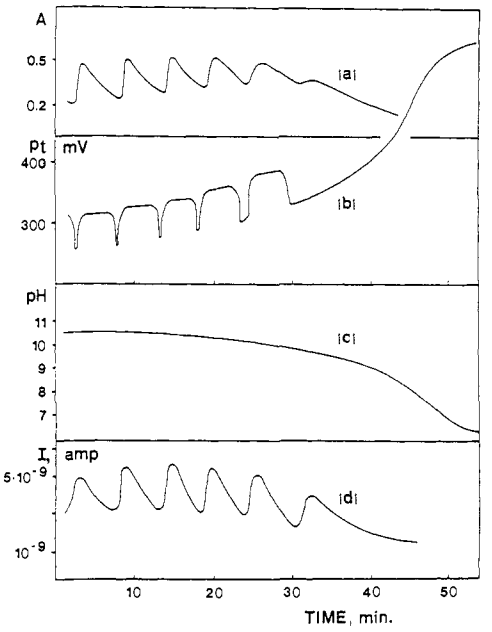


**Figure 1.** Experimentally determined batch behavior[8] in the oscillatory $H_2O_2$–KSCN–Cu(II) system. Initial concentrations: $[H_2O_2]_0 = 0.25$ M, $[KSCN]_0 = 0.0375$ M, $[NaOH]_0 = 0.025$ M, $[CuSO_4]_0 = 7.5 \times 10^{-5}$ M. Temperature 25 °C. (a) Absorbance at 375 nm, cell width 2 cm; (b) potential of Pt electrode against $Hg|Hg_2SO_4|K_2SO_4$ reference electrode; (c) pH; (d) ionic current in amperes recorded with mass spectrometer for the species of mass number 32. The ionic current is proportional to the partial pressure of oxygen evolved in and driven out of the reaction mixture.

FKN mechanism[9] for the classic Belousov–Zhabotinskii (BZ) reaction, which has greatly enriched oxybromine chemistry and has served as the basis for an entire family of bromate-driven oscillators.

The mechanism presented here simulates nearly all the dynamic behavior of the alkaline $H_2O_2$–KSCN–$CuSO_4$ system observed experimentally, including slowly damped oscillation in color and oxygen evolution accompanied by a monotonic pH change under closed conditions, sustained oscillation in flow, and bistability between the two steady states and between one steady state and the oscillatory state.

Our mechanism is derived from careful mechanistic studies for the two subsystems: the oxidation of potassium thiocyanate by hydrogen peroxide[10] and the decomposition of hydrogen peroxide catalyzed by $CuSO_4$ in strongly alkaline media.[11] These studies were able to account for the stoichiometry and the overall kinetics of the two separate subsystems. However, simply putting together the reactions in these two mechanisms and taking into account complex formation between copper and thiocyanate ions does not lead to a mechanism capable of oscillatory behavior for any set of rate constants. It became apparent that more intermediate species need to be invoked to construct sufficient feedback cycles to permit oscillation.

As detailed below, the intermediates we propose are cyanosulfite, $^-OS(O)CN$, and peroxocyanosulfite, $^-OOS(O)CN$, ions as well as the hypothiocyanite ion, $^-OSCN$, and the peroxohypothiocyanate ion, $^-OOSCN$, used in Wilson and Harris's mechanism[10] for the oxidation of $SCN^-$ by $H_2O_2$. We discuss in the last section other sets of intermediates that can give rise to oscillatory behavior. The mechanism chosen appears most reasonable in terms of the plausibility of the intermediates, the elementary reactions, and the rate constants. It also gives better agreement with the experiments in the shape and frequencies of oscillation, as well as multistable behavior under flow conditions. Nevertheless, as we shall describe, the present mechanism is far from giving complete agreement with all aspects of the system's dynamical behavior.

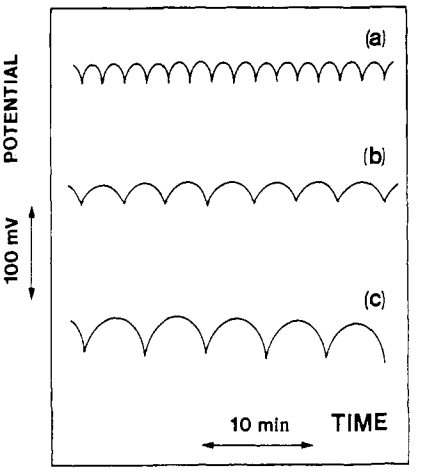


**Figure 2.** Sustained oscillation in Pt potential at different flow rates in a CSTR.[8] Input concentrations: $[H_2O_2]_0 = 0.25$ M, $[KSCN]_0 = 0.025$ M, $[NaOH]_0 = 0.025$ M, $[Cu(II)]_0 = 5 \times 10^{-5}$ M. Flow rates: (a) $8.1 \times 10^{-3}$ s$^{-1}$; (b) $2.7 \times 10^{-3}$ s$^{-1}$; (c) $1.0 \times 10^{-3}$ s$^{-1}$.

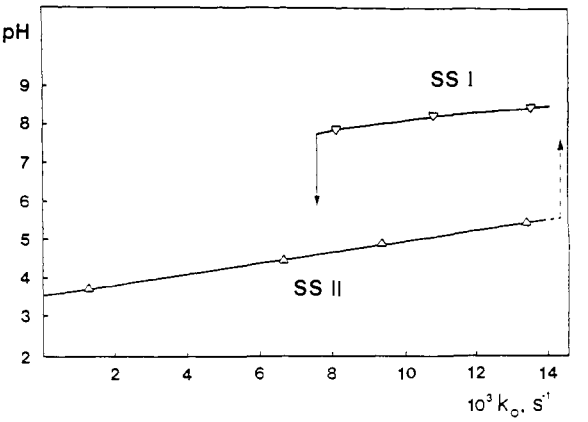


**Figure 3.** Hysteresis between SSI and SSII in the CSTR[8] with input concentrations $[H_2O_2]_0 = 0.25$ M, $[KSCN]_0 = 0.025$ M, $[NaOH]_0 = 0.001$ M, $[CuSO_4]_0 = 5 \times 10^{-5}$ M. Dashed line shows the pH change in the absence of Cu(II).

## Experimental Background

Under basic conditions, the two subsystems $H_2O_2$–KSCN[10] and $H_2O_2$–$CuSO_4$[11] were shown to behave monotonically and did not show evidence of strong autocatalysis. The oxidation of KSCN by $H_2O_2$ in alkaline solution is very slow.[8,10] The final products are sulfate, bicarbonate, and ammonium ions. The reaction pathway is thought to involve oxygen transfer from hydrogen peroxide to thiocyanate followed by bond cleavage between the sulfur and the cyanide and finally between the carbon and the nitrogen.[10] There is weak acid catalysis at low pH, producing a small amount of HCN.

The decomposition of hydrogen peroxide to oxygen and water catalyzed by cupric ion is much faster in strongly alkaline than in acidic media. The formation of a yellow superoxide–cuprous complex, $HO_2$–Cu(I), which exists only at pH ≥ 9, plays a crucial role in determining the pathway of copper catalysis under different pH conditions.[11]

When the three components of the present system are mixed in batch (no material fluxes), as done by Orbán,[8] the rate of oxidation of KSCN by $H_2O_2$ increases moderately, but the decomposition of $H_2O_2$ is largely hindered. At a sufficiently high initial pH with appropriate reagent concentrations, a most surprising phenomenon is observed: oxygen evolution, the appearance and disappearance of a yellow color and increases and decreases in the potential of a Pt electrode take place periodically, while the pH decreases slowly and monotonically. The oscillation ceases when the pH falls below 9, where the yellow peroxo–cuprous complex is no longer able to form. The experimental batch oscillations[8] are shown in Figure 1.

(9) Noyes, R. M.; Field, R. J.; Körös, E. *J. Am. Chem. Soc.* **1972**, *94*, 1394.

(10) Wilson, I. R.; Harris, G. M. *J. Am. Chem. Soc.* **1960**, *82*, 4515. Wilson, I. R.; Harris, G. M. *J. Am. Chem. Soc.* **1961**, *83*, 286.

(11) Luo, Y.; Kustin, K.; Epstein, I. R. *Inorg. Chem.* **1988**, *27*, 2489. Reactions 1-10 and the nature of the copper–peroxide species are discussed in detail in this reference.

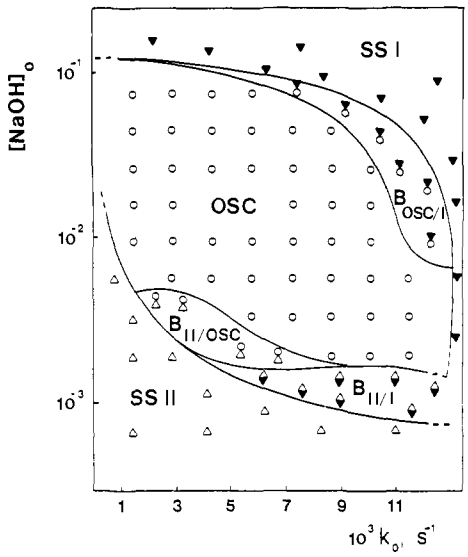


**Figure 4.** Phase diagram for the $H_2O_2$–KSCN–Cu(II) system in the $[NaOH]_0$–$k_0$ plane.[8] Fixed constraints are the same as in Figure 3: ▽, SSI; △, SSII; ○, oscillations. Combinations of the above symbols imply multistability among the corresponding modes.

The $H_2O_2$–KSCN–$CuSO_4$ system shows sustained oscillation in a continuously stirred tank reactor (CSTR[8]), Figure 2. Under different conditions two steady states are found in the CSTR: SSI at high (8–10) pH and SSII at low (4–6.5) pH. Bistability between the two steady states is observed at lower $[NaOH]_0$, Figure 3. Bistability between SSI and the oscillatory state and between SSII and the oscillatory state is also found, indicating the complexity of the system's dynamics. The three kinds of bistability and the conditions under which they occur are summarized in the flow rate ($k_0$)–$[NaOH]_0$ phase diagram of Figure 4.

## Mechanism

**$H_2O_2$–$CuSO_4$ Subsystem.** The kinetics of the Cu(II)-catalyzed decomposition of hydrogen peroxide were studied by Luo et al.[11] in alkaline medium. A mechanism was proposed involving five fast equilibria and five kinetic steps in the pH range 11–12: see eq 1–10, where R = $[HO_2^{\bullet}] + [O_2^{\bullet-}]$. The equilibrium and rate

$$H_2O_2 + HO^- \leftrightarrow HO_2^- + H_2O \quad K_1 \qquad (1)$$

$$Cu^{2+} + HO_2^- + 3\,OH^- \leftrightarrow O_2Cu(OH)_2^{2-} + H_2O \quad K_2 \qquad (2)$$

$$Cu^{2+} + H_2O_2 + 3\,OH^- \leftrightarrow HO_2Cu(OH)_2^- + H_2O \quad K_3 \qquad (3)$$

$$Cu^{2+} + 3\,OH^- \leftrightarrow Cu(OH)_3^- \quad K_4 \qquad (4)$$

$$Cu^{2+} + 4\,OH^- \leftrightarrow Cu(OH)_4^{2-} \quad K_5 \qquad (5)$$

$$O_2Cu(OH)_2^{2-} \rightarrow Cu(OH)_2^- + O_2^{\bullet-} \quad k_6 \qquad (6)$$

$$HO_2Cu(OH)_2^- \rightarrow Cu(OH)_2^- + HO_2^{\bullet} \quad k_{6'} \qquad (6')$$

$$Cu(OH)_2^- + O_2 + OH^- \rightarrow Cu(OH)_3^- + O_2^{\bullet-} \quad k_7 \qquad (7)$$

$$Cu(OH)_2^- + H_2O_2 \rightarrow Cu(OH)_3^- + OH^{\bullet} \quad k_8 \qquad (8)$$

$$Cu(OH)_2^- + HO_2^- \rightarrow Cu(OH)_3^- + OH^{\bullet} + OH^- \quad k_{8'} \qquad (8')$$

$$OH^{\bullet} + H_2O_2 \rightarrow H_2O + HO_2^{\bullet} \quad k_9 \qquad (9)$$

$$OH^{\bullet} + HO_2^- \rightarrow H_2O + O_2^{\bullet-} \quad k_{9'} \qquad (9')$$

$$R + R \rightarrow H_2O_2\,(HO_2^-) + O_2\,(+OH^-) \quad k_{10} \qquad (10)$$

constants[11] are summarized in Table I. The yellow superoxo–Cu(I) complex ($HO_2$–Cu(I) represents both $HO_2Cu(OH)_2^-$ and $O_2Cu(OH)_2^{2-}$) was identified as the key species in the reaction in strongly alkaline medium. Its apparent formation constant, $K_{app}$, is highly pH dependent (eq 11). Other equilibria of cop-

$$K_{app} = (K_1K_2[OH^-]^4 + K_3[OH^-]^3)/(1 + K_1[OH^-]) \qquad (11)$$

per–hydroxide complexes are competitive with the formation of $HO_2$–Cu(I). The unimolecular decomposition of $HO_2$–Cu(I) to copper(I) and superoxide radical is rate determining. Only lower bounds and the ratio of the rate constants for copper(I) reoxidation by dioxygen and hydrogen peroxide ($k_7$ and $k_8$) were estimated; the overall kinetic behavior is not sensitive to the actual values of these rate constants. The superoxide radical serves as a precursor for molecular oxygen formation rather than an active intermediate or a catalyst.

Table I. Equilibrium and Rate Constants for the Alkaline Decomposition of $H_2O_2$ Catalyzed by Copper(II)[a]

| constant | value |
|---|---|
| $K_1$ | $2.4 \times 10^2$ |
| $K_2$ | $<4.8 \times 10^{17}$ $M^{-4}$ |
| $K_3$ | $<3.3 \times 10^{17}$ $M^{-4}$ |
| $K_4$ | $<1.6 \times 10^{14}$ $M^{-3}$ |
| $K_5$ | $<2.5 \times 10^{16}$ $M^{-4}$ |
| $k_6$ | $2.54 \times 10^{-2}$ $s^{-1}$ |
| $k_6'$ | $6.93 \times 10^{-3}$ $s^{-1}$ |
| $k_7$ | $3.3 \times 10^9$ $M^{-1}$ $s^{-1}$ |
| $k_8 = k_8'$ | $5 \times 10^{-5} \times 10^9$ $M^{-1}$ $s^{-1}$ |
| $k_9 = k_9'$ | $1.02 \times 10^9$ $M^{-1}$ $s^{-1}$ |
| $k_{10}$ | $(7.61 \times 10^5 + 1.57 \times 10^3/[H^+])/((1 + 1.78 \times 10^{-5}/[H^+])^2)$ $M^{-1}$ $s^{-1}$ |

[a] From ref 11.

**$H_2O_2$–KSCN Subsystem.** Wilson and Harris[10] investigated the stoichiometry of the reaction in both alkaline and acidic conditions. In alkaline media they found

$$4H_2O_2 + SCN^- \rightarrow HSO_4^- + HOCN + 3H_2O \qquad (12)$$

$$HOCN + 2H_2O \rightarrow NH_4^+ + HCO_3^- \qquad (13)$$

while in acidic media

$$3H_2O_2 + SCN^- \rightarrow HSO_4^- + HCN + 2H_2O \qquad (14)$$

They suggested a stepwise mechanism (eq 15–21) for the reaction.

$$SCN^- + H_2O_2 \rightarrow HOSCN + OH^- \quad (pH > 4) \quad k_{15} \qquad (15)$$

$$HOSCN + H_2O_2 \rightarrow HOOSCN + H_2O \quad k_{16} \qquad (16)$$

$$HOOSCN + H_2O_2 \rightarrow H_2SO_3 + HOCN \quad (pH > 4) \quad k_{17} \qquad (17)$$

$$H_2SO_3 + H_2O_2 \rightarrow H_2SO_4 + H_2O \quad k_{18} \qquad (18)$$

$$HOCN + 2H_2O \rightarrow HCO_3^- + NH_4^+ \quad k_{19} \qquad (19)$$

$$H^+ + SCN^- + H_2O_2 \rightarrow HOSCN + H_2O \quad (pH < 4) \quad k_{20} \qquad (20)$$

$$H_3O^+ + HOOSCN \rightarrow H_2SO_3 + HCN + H^+ \quad (pH < 4) \quad k_{21} \qquad (21)$$

Hypothiocyanous acid or hydroxythiocyanate, HOSCN, and peroxohypothionous acid, HOOSCN, are postulated as short-lived intermediates. Sulfite oxidation by hydrogen peroxide is fast enough[12] that the sulfite concentration remains very low. The measured rates of disappearance of $H_2O_2$ or $SCN^-$ were assigned as the rates of the assumed rate-determining steps, (15) and (20): $k_{15} = 4.0 \times 10^9 \exp(-15500/RT)$ $M^{-1}$ $min^{-1}$, $k_{20} = 1.75 \times 10^8 \exp(-11000/RT)$ $M^{-2}$ $min^{-1}$, ($R$ = 1.987 cal $mol^{-1}$ $K^{-1}$) in the temperature range 20–50 °C. Other rate constants were left undetermined, except $k_{19}$, which can be estimated to some extent from literature values.[13]

This reaction is of much interest in biochemistry and has been studied under enzyme catalysis.[14-16] The relatively stable hypothiocyanate ion, $OSCN^-$, was found to oxidize sulfhydryl compounds to disulfide compounds and to regenerate thiocyanate:[16]

$$OSCN^- + 2RSH \rightarrow SCN^- + RSSR + H_2O \qquad (22)$$

(12) Mader, P. M. *J. Am. Chem. Soc.* **1958**, *80*, 2634.
(13) Jensen, M. B. *Acta Chem. Scand.* **1958**, *12*, 1657.
(14) Oram, J. D.; Reiter, B. *Biochem. J.* **1966**, *100*, 382.
(15) Hogg, D. McC.; Jago, G. R. *Biochem. J.* **1970**, *117*, 779.
(16) Aune, T. M.; Thomas, E. L. *Eur. J. Biochem.* **1977**, *80*, 209.

More structurally distinguished intermediates, HOS(O)CN and $HOS(O)_2CN$, were proposed,[15] though neither was detected directly. They were shown indirectly, however, to be short-lived in water.[17]

**$H_2O_2$–KSCN–$CuSO_4$ System.** The mechanism for the oscillatory $H_2O_2$–KSCN–$CuSO_4$ system presented here is composed of 30 kinetic reactions using 26 independent variables. These reactions are more easily grasped in groups, each containing reactions specific to one part of the overall reaction.

Most of the reactions in the first two groups are adopted from the mechanisms for the two subsystems. However, much alteration is necessary to keep the mechanism as simple as possible, to make it applicable over a much larger pH range, and to provide the essential intermediates for the oscillatory network. The third group is the centerpiece of the mechanism. It contains the machinery of the oscillation: the positive and negative feedback loops. The fourth group generates the low pH steady state (SSII) and its bistability with the high pH steady state (SSI). We discuss the details of each group below.

1. Reactions between $H_2O_2$ and $Cu^{2+}$:

$$H_2O_2 + Cu^{2+} + OH^- \leftrightarrow HO_2\text{–}Cu(I) + H_2O \qquad k_{M1}, k_{M2} \quad (M1, M2)$$

$$HO_2\text{–}Cu(I)\ [+n SCN^-] \rightarrow Cu^+\{SCN^-\}_n + HO_2^\bullet \qquad k_{M3} \quad (M3)$$

$$2HO_2^\bullet \rightarrow H_2O_2 + O_2 \qquad k_{M4} \quad (M4)$$

where $n$ may be 2, 3, or 4.

Only four reactions are chosen from the 10-step mechanism in ref 11 (eq 1–10). The hydrolysis of $Cu^{2+}$ ion (eq 4 and 5) is omitted, because these equilibria are significant only in the pH range 11–12. The full reaction with KSCN, however, stays in that pH range for only a very short period even if it starts at pH 12, and it quickly undergoes a change to lower pH. In addition, the majority of the experiments shown in Figure 4 have an initial pH < 12. For the same reason the deprotonation equilibrium of $H_2O_2$, eq 1, is neglected, which allows us to simplify the formation and the decomposition of the superoxide–copper(I) complexes as (M1), (M2), and (M3). Reaction 10 then also simplifies to (M4), in which only the protonated species are included. A simplified reaction (eq 9) will appear in group 4.

These four reactions are chosen both to represent the major effects of the copper-catalyzed alkaline $H_2O_2$ decomposition in the mixed reaction and to provide two essential intermediates, $HO_2^\bullet$ and $Cu^+\{SCN^-\}_n$, for the core part of the oscillation. The use of braces will be explained in the section on numerical simulation.

The stability constant for the copper(II)–thiocyanate complex is at least 10 orders of magnitude less than that for $HO_2$–Cu(I).[11,18] The former complex is therefore omitted from the mechanism. On the other hand, the Cu(I) complex, $Cu(SCN)_n^-$, is extremely stable, with $K_s > 10^{11}$ $M^{-2}$ (ref 18) for $n = 2$, and no other copper(I) complex can compete under these conditions. On the basis of the fact that $SCN^-$ causes the yellow color of the solution to fade and retards the evolution of $O_2$, we postulate that $SCN^-$ strongly complexes $Cu^+$ after it is formed from the decomposition of $HO_2$–Cu(I), preventing the copper from immediate reoxidation by $O_2$ or $H_2O_2$ (eq 7 and 8). The sharp increase in color and $O_2$ evolution that occur in the oscillation cycle then result from autocatalytic reactions among the active intermediates to be described in group 3. The lack of color of the high-flow steady-state SSI in the CSTR supports this interpretation. Taking these assumptions still further, the mechanism is greatly simplified by assigning all $Cu^+$ as $Cu(SCN)_2^-$, by neglecting the complexation equilibrium, and by disregarding the oxidation of the $Cu^+$ complex by $O_2$ or $H_2O_2$.

The values of all rate constants are listed in Table II. The rate constant $k_{M1}$ is taken as $1.0 \times 10^5$ $M^{-2}$ $s^{-1}$ on the basis of the observation of fast complex formation.[11] The ratio $k_{M1}/K_{app}$ is used to calculate $k_{M2}$ with eq 11, which is updated with a new value of $[OH^-]$ at each call to the numerical integration program. Rate constant $k_{M3}$ is roughly the average of $k_6$ and $k_{6'}$, and $k_{M4}$ is chosen to be equal to $k_{10}$ at a pH between 11 and 12.

Table II. Rate Constants in the Mechanism for $H_2O_2$–KSCN–Cu(II)

| constant | value | constant | value |
|---|---|---|---|
| $k_{M1}$ | $1.0 \times 10^5$ $M^{-2}$ $s^{-1}$ | $k_{M2}$ | $k_{M1}/K_{app}$ [a] |
| $k_{M3}$ | $1.0 \times 10^{-2}$ $s^{-1}$ | $k_{M4}$ | $2.0 \times 10$ $M^{-1}$ $s^{-1}$ |
| $k_{M5}$ | $7.5 \times 10^{-4}$ $M^{-1}$ $s^{-1}$ | $k_{M6}$ | $3.0 \times 10^{-1}$ $M^{-1}$ $s^{-1}$ |
| $k_{M7}$ | $5.0 \times 10^2$ $M^{-1}$ $s^{-1}$ | $k_{M8}$ | $1.0 \times 10^3$ $M^{-1}$ $s^{-1}$ |
| $k_{M9}$ | 1.0 $M^{-1}$ $s^{-1}$ | $k_{M10}$ | $1.0 \times 10^{-1}$ $s^{-1}$ |
| $k_{M11}$ | $1.0 \times 10^{-3}$ $s^{-1}$ | $k_{M12}$ | $5.0 \times 10^{-2}$ $s^{-1}$ [b] |
| $k_{M13}$ | $1.0 \times 10^9$ $M^{-1}$ $s^{-1}$ | $k_{M14}$ | $2.51 \times 10$ $s^{-1}$ [b] |
| $k_{M15}$ | $1.0 \times 10^9$ $M^{-1}$ $s^{-1}$ | $k_{M16}$ | $1.62 \times 10^6$ $s^{-1}$ [b] |
| $k_{M17}$ | $1.0 \times 10^9$ $M^{-1}$ $s^{-1}$ | $k_{M18}$ | $3.0 \times 10^3$ $M^{-1}$ $s^{-1}$ |
| $k_{M19}$ | $2.0 \times 10^6$ $M^{-1}$ $s^{-1}$ | $k_{M20}$ | $1.0 \times 10^5$ $M^{-1}$ $s^{-1}$ |
| $k_{M21}$ | $2.0 \times 10^3$ $M^{-1}$ $s^{-1}$ | $k_{M22}$ | $1.5 \times 10^5$ $M^{-1}$ $s^{-1}$ |
| $k_{M23}$ | $1.0 \times 10^8$ $M^{-1}$ $s^{-1}$ | $k_{M24}$ | $2.0 \times 10^{-1}$ $M^{-1}$ $s^{-1}$ |
| $k_{M25}$ | $1.0 \times 10^6$ $M^{-1}$ $s^{-1}$ | $k_{M26}$ | $1.0 \times 10^9$ $M^{-2}$ $s^{-1}$ |
| $k_{M27}$ | $5.0 \times 10^6$ $M^{-1}$ $s^{-1}$ | $k_{M28}$ | $1.0 \times 10^3$ $M^{-1}$ $s^{-1}$ |
| $k_{M29}$ | $3.0 \times 10^1$ $M^{-1}$ $s^{-1}$ | $k_{M30}$ | $2.0 \times 10^9$ $M^{-1}$ $s^{-1}$ |

[a] For expression for $K_{app}$, see text. [b] Calculated from the equilibrium constants in ref 18.

2. Reactions between $H_2O_2$ and KSCN:

$$H_2O_2 + SCN^- \rightarrow {}^-OSCN + H_2O \qquad k_{M5} \quad (M5)$$

$$H_2O_2 + {}^-OSCN \rightarrow {}^-OOSCN + H_2O \qquad k_{M6} \quad (M6)$$

$$2\,{}^-OOSCN \rightarrow {}^-OOS(O)CN + {}^-OSCN \qquad k_{M7} \quad (M7)$$

$${}^-OOSCN + {}^-OOS(O)CN\ [+OH^-] \rightarrow {}^-OSCN + SO_4^{2-} + HOCN \qquad k_{M8} \quad (M8)$$

$$2\,{}^-OOS(O)CN\ [+OH^-] \rightarrow {}^-OS(O)CN + SO_4^{2-} + HOCN \qquad k_{M9} \quad (M9)$$

$$HOCN + 2H_2O \rightarrow HCO_3^- + NH_4^+ \qquad k_{M10} \quad (M10)$$

$${}^-OCN + 2H_2O \rightarrow HCO_3^- + NH_3 \qquad k_{M11} \quad (M11)$$

$${}^-OCN + H_2O \leftrightarrow HOCN + OH^- \qquad k_{M12}, k_{M13} \quad (M12, M13)$$

$$HCO_3^- + H_2O \leftrightarrow H_2CO_3 + OH^- \qquad k_{M14}, k_{M15} \quad (M14, M15)$$

$$NH_3 + H_2O \leftrightarrow NH_4^+ + OH^- \qquad k_{M16}, k_{M17} \quad (M16, M17)$$

The use of brackets for some of the $OH^-$ will be explained in the section on numerical simulation.

This group of reactions provides a complete route for the oxidation of $SCN^-$ to the final products. It is derived from Wilson and Harris's work[10] but augments their mechanism by including more intermediates. The reason for this addition is to provide sufficient degrees of freedom for the next group of reactions to construct a plausible feedback loop that generates oscillatory behavior even under batch conditions when copper ion is included.

The first step of thiocyanate oxidation to hypothiocyanite ion, (M5), is still the rate-determining step of this part of the reaction. The equilibrium constant for the deprotonation of HOSCN is not known. On the basis of the similarity of $SCN^-$ to halide, and for convenience, we choose to use the anion forms for all the oxidized thiocyanate intermediates. The rate constant for this reaction is taken to be very close to the non-acid-catalyzed overall reaction rate measured by Wilson and Harris.[10]

The second step, (M6), is considered to resemble a ligand-exchange reaction, in which $HOO^-$ replaces $OH^-$. This reaction should therefore be faster than (M5), which requires O–O bond breaking. The $^-OOSCN$ ion is then explicitly defined as a peroxohypothiocyanate ion, It differs from $^-OS(O)CN$, which we refer to as a cyanosulfite ion, in which the oxygen in parentheses is double bonded to the sulfur.

Reactions M7, M8, and M9 take account of two empirical observations: (1) oxygen transfers between sulfur species are

(17) Jander, G.; Grattner, B.; Scholz, G. *Chem. Ber.* **1947**, *80*, 279.
(18) Sillén, L. G.; Martell, A. E. *Chem. Soc. Spec. Publ.* **1964**, *No. 17*.

usually rapid; (2) the higher the oxidation state of a sulfur species, the higher its affinity for additional oxygens. Again, in $^-$OOS(O)CN, peroxocyanosulfite ion, the sulfur is singly bonded to superoxide and doubly bonded to oxygen. The rate constants for these proposed reactions, listed in Table II, were estimated on the basis of the above rules and then refined by fitting the simulations to the oscillation experiments.

The three fast equilibria are necessary because the species involved are present in high concentrations during some stage of the reaction and because the relevant p$K_a$'s lie between the pH's of the two steady states. In the absence of experimental data, the rate constant for the bimolecular direction of each equilibrium has been taken at or near the diffusion limit, and that of the monomolecular direction estimated from the individual equilibrium constant.[18]

The hydrolysis of $^-$OCN is known to be very slow in basic media and to show acid catalysis.[13] However, no quantitative measurement has been done on this reaction in conditions close to those of the oscillation. The values of $k_{M10}$ and $k_{M11}$ used in the calculations are crude estimates.

3. Feedback networks:

$$^-OS(O)CN + {}^-OOS(O)CN + H_2O \leftrightarrow 2{}^\bullet OS(O)CN\ [+2OH^-] \quad k_{M18}, k_{M19} \quad (M18, M19)$$

$$^\bullet OS(O)CN + Cu^+\{SCN^-\}_n \rightarrow {}^-OS(O)CN + Cu^{2+}\{+nSCN^-\} \quad k_{M20} \quad (M20)$$

$$^-OS(O)CN + HO_2^\bullet \rightarrow SO_3^{\bullet-} + HOCN \quad k_{M21} \quad (M21)$$

$$SO_3^{\bullet-} + Cu^+\{SCN^-\}_n \rightarrow SO_3^{2-} + Cu^{2+}\{+nSCN^-\} \quad k_{M22} \quad (M22)$$

$$2SO_3^{\bullet-}\ [+2OH^-] \rightarrow SO_4^{2-} + SO_3^{2-} + H_2O \quad k_{M23} \quad (M23)$$

$$H_2O_2 + SO_3^{2-} \rightarrow SO_4^{2-} + H_2O \quad k_{M24} \quad (M24)$$

Only intermediates and Cu(II), but no input reagents, appear on the right-hand side of this group of reactions—a fact that ensures that if the mechanism can oscillate under flow conditions, it is likely to oscillate in batch as well. This features also explains why even though neither of the subsystems is autocatalytic, the system oscillates when they are mixed.

The autocatalysis, a positive feedback loop in this case, is accomplished by the sequence (M18, M19) + 2(M20), involving two intermediates from the second group, $^-$OS(O)CN and $^-$OOS(O)CN, and one from the first group, the $Cu^+$–thiocyanate complex. Intermediate $^-$OS(O)CN is produced very slowly in reaction M9, and it initially has a very low concentration. It is generated autocatalytically through the formation and reduction of the radical $^\bullet$OS(O)CN, when the concentrations of $^-$OS(O)CN and $Cu^+\{SCN^-\}_n$ become high enough to make this pathway significant. The $Cu^+$ is simultaneously oxidized to $Cu^{2+}$, and the fast equilibrium, (M1) and (M2), produces the yellow superoxy complex almost immediately if the system is in the appropriate pH range. The sharp increase in color stops when most of the $Cu^+$ has been consumed.

To bring the system back to the state it was in prior to the autocatalysis, so that the above process can start again, a negative feedback, i.e., a process that is activated as a result of the positive feedback but that functions in the opposite direction, is required. In the present mechanism, the negative feedback pathway is composed of three reactions, (M21), (M22), and (M23)). Keeping in mind that the formation and the decomposition of the $HO_2$–Cu(I) complex are both rapid, we know that $HO_2^\bullet$ builds up as sharply as the absorbance, but with a very brief delay. With an appropriate $k_{M21}$, the autocatalytic species, $^-$OS(O)CN, is consumed by $HO_2^\bullet$ when both species reach sufficient levels, and the first turning point of the oscillation occurs. However, the monomolecular decomposition (M3) produces $Cu^+\{SCN^-\}_n$ simultaneously with $HO_2^\bullet$. The former species can reinitiate the positive feedback pathway, and since the process is autocatalytic the system would be prevented from returning to the original state. Step M22 ensures that $[Cu^+\{SCN^-\}_n]$ is maintained at a low level until $SO_3^{\bullet-}$ is exhausted, i.e., when $^-$OS(O)CN is consumed. This phase-shift control step is as crucial as the direct competition for the autocatalytic species between the positive and negative feedback processes. The disproportionation of the $SO_3^{\bullet-}$ radical (M23) is included for completeness, though it does not play an essential role.

Not surprisingly, none of the rate constants in this group, except $k_{M24}$, can be found in the literature. The values listed in Table II have all been fitted to give the best agreement with the oscillation experiments. They are certainly subject to further improvement as discussed below. Reaction M24 is fast enough[12] to keep $[SO_3^{2-}]$ well below the concentrations of the major products, so that inclusion of its equilibrium with $HSO_3^-$ is not expected to make a significant difference, even though the p$K_a$ is 7.2.[19]

4. Acid-producing reactions (low-pH steady state):

$$^-OOSCN + H^+ + H_2O \rightarrow SO_3^{2-} + HCN + 2H^+ \quad k_{M25} \quad (M25)$$

$$Cu^{2+} + 2HCN \rightarrow Cu(CN)_2 + 2H^+ \quad k_{M26} \quad (M26)$$

$$2Cu(CN)_2 \rightarrow 2Cu(CN) + (CN)_2 \quad k_{M27} \quad (M27)$$

$$H_2O_2 + (CN)_2 \rightarrow 2HOCH \quad k_{M28} \quad (M28)$$

$$H_2O_2 + Cu(CN) + H_2O \rightarrow Cu^{2+} + 2OH^- + OH^\bullet + HCN \quad k_{M29} \quad (M29)$$

$$H_2O_2 + OH^\bullet \rightarrow HO_2^\bullet + H_2O \quad k_{M30} \quad (M30)$$

This group of reactions comes into play when the pH is $\leq 7$ to bring the system to the lower pH of steady state II when the flow rate is sufficiently low. It does not have any effect on either oscillatory state or the high-pH steady state I.

The first reaction is taken directly from Wilson and Harris' mechanism,[10] with the rate constant fitted to the oscillation experiment. Another acid-catalyzed reaction in that mechanism, eq 20, is not included here, since it becomes comparable to the non-acid-catalyzed reaction, (M5), only as the pH approaches 1.[10]

Reactions M26 and M27 involving copper ion catalysis correspond to the familiar analytical reaction in which $Cu^{2+}$ is reduced by HCN to a very stable complex, Cu(CN), with accompanying production of $(CN)_2$.[20] Steps M29 and M30 are analogous to reactions in the mechanism for the $H_2O_2$–$CuSO_4$[11] reaction. We now take into consideration the oxidation of the copper(I) complex by $H_2O_2$, because $H_2O_2$ is a good oxidant in acidic medium, though it behaves as a reductant in strong alkaline media. For simplicity, competition between the thiocyanate and cyanide complexes of copper(I) is not taken into account, even though the complexes have stability constants of similar magnitude.[18] All rate constants in this group, except the diffusion-controlled $k_{M30}$,[21] are fitted numbers.

### Numerical Simulation and Results

All reactants and intermediates, 26 in total, that appear on the left-hand side of eq M1–M30, except $H^+$, are taken as independent variables. We replace $[H^+]$ by $10^{-14}/[OH^-]$ in the rate law for reaction M25. The $H^+$ production in (M25) and (M26) is taken into account stoichiometrically by subtracting one $OH^-$ for every $H^+$ produced. With the exception of (M1) and (M26), all reactions have unimolecular or bimolecular kinetics. The $OH^-$'s in brackets in (M8), (M9), (M19), and (M23) are taken into account in the stoichiometry but do not enter into the rate laws of these reactions. The underlying assumption is that these reactions are not elementary steps and that fast protonation or deprotonation follows the rate-determining bimolecular step to yield the indicated products. A similar assumption is made in

(19) *Lange's Handbook of Chemistry*, 11th ed.; Dean, J. A., Ed.; McGraw-Hill: New York, 1973; pp 5–15.
(20) Hogness, T. R.; Johnson, W. C. *Qualitative Analysis and Chemical Equilibrium*, 4th ed.; Henry Holt & Co.: New York, 1954; p 401.
(21) Keyser, L. F.; Choo, K. Y.; Leu, M. T. *Int. J. Chem. Kinet.* **1985**, *17*, 1169.

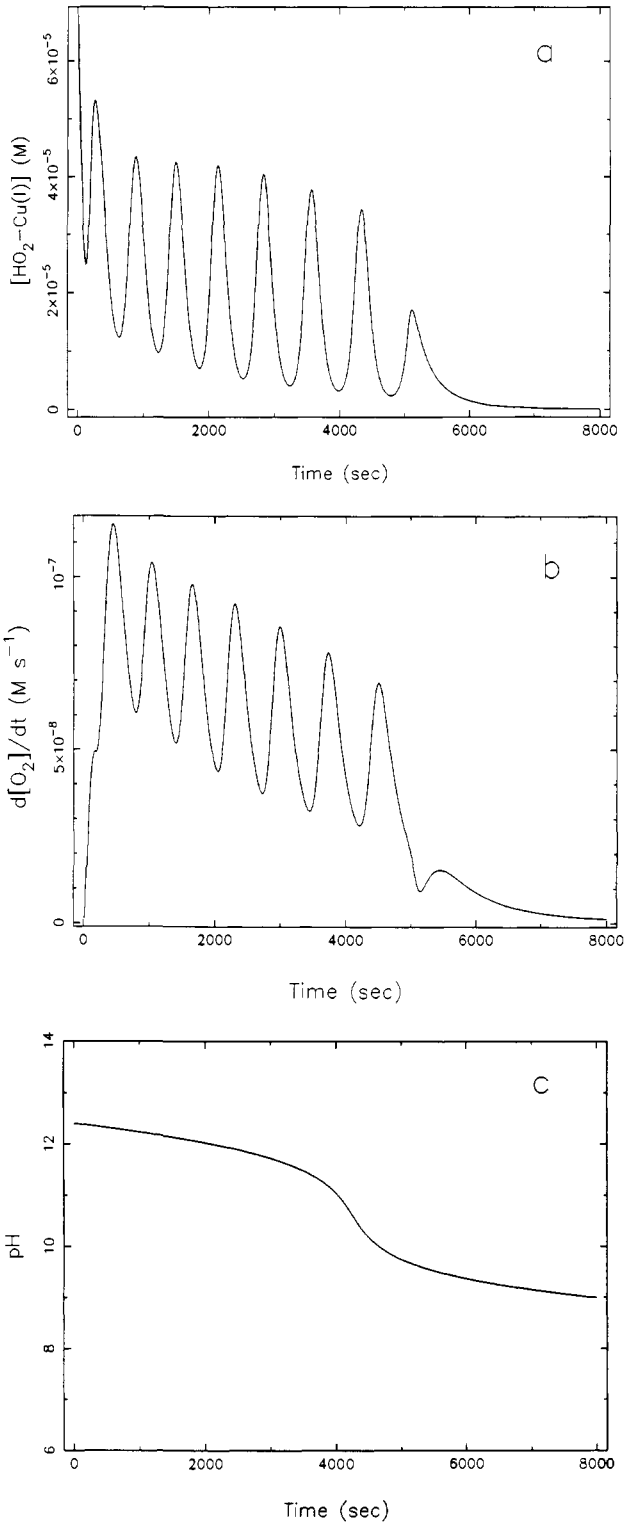


**Figure 5.** Calculated batch oscillations in (a) $[HO_2–Cu(I)]$ and (b) $d[O_2]/dt$ and monotonic pH curve (c) during the same time interval. Initial conditions: $[H_2O_2]_0 = 0.25$ M, $[KSCN]_0 = 0.025$ M, $[NaOH]_0 = 0.025$ M, $[CuSO_4]_0 = 7.5 \times 10^{-5}$ M.

the case of $SCN^-$ bound to copper ion. However, for simplicity, the $SCN^-$'s in braces in (M3), (M20), and (M22) are not even included in the stoichiometry. They are dummy symbols here to show the sense of the chemistry.

The resulting set of 26 differential equations was integrated numerically with the Gear package.[22] The calculated $[HO_2–Cu(I)]$ may be compared with the experimental absorbance. The calculated rate of $O_2$ production, $d[O_2]/dt$, should correspond, at least qualitatively, to the $O_2$ evolution (in terms of current) measured with the mass spectrometer.[8]

(22) Gear, C. W. *Numerical Initial Value Problems in Ordinary Differential Equations*; Prentice-Hall: Englewood Cliffs, NJ, 1971.

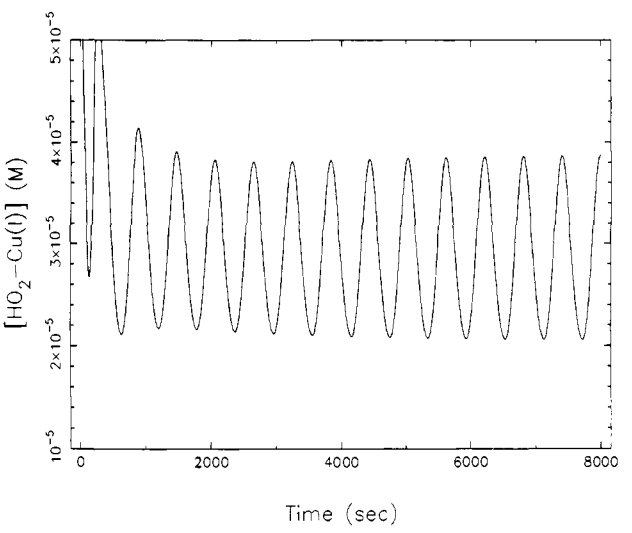


**Figure 6.** Calculated oscillations under flow conditions: $k_0 = 1.0 \times 10^{-3}$ $s^{-1}$. Initial (in-flow) concentrations are the same as in Figure 5.

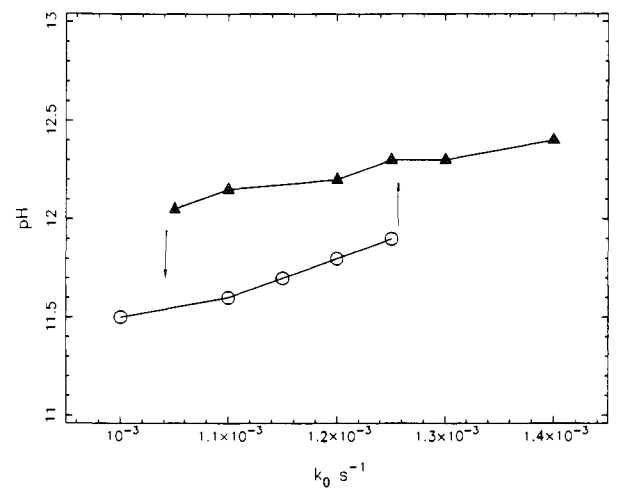


**Figure 7.** Calculated hysteresis between SSI (△) and oscillatory state (○, in which the pH is constant). All initial (in-flow) concentrations are the same as in Figure 5.

**Batch Oscillation.** With considerable computational effort in matching so many free parameters (rate constants), we have been able to simulate the damped oscillation seen in a closed system (zero flow rate) with the mechanism (M1)–(M30) and the rate constants listed in Table II with initial conditions identical with those of the experiments (Figure 1). The calculated oscillations in $[HO_2–Cu(I)]$ and $d[O_2]/dt$ are illustrated in Figure 5. The period agrees with the experiment to within a factor of 2. The shape of the $d[O_2]/dt$ oscillation resembles that of the experimental $O_2$ evolution (Figure 1d). The magnitude of the $[HO_2–Cu(I)]$ oscillation is consistent with the measured absorbance change, according to the estimated extinction coefficient of the $HO_2–Cu(I)$ complex.[11] In agreement with the experimental findings, $[OH^-]$ shows a slow monotonic change over the course of the oscillation, which terminates when the pH approaches 9 (see Figure 1).

**Oscillation and Bistability in Flow.** The mechanism gives oscillation when the flow is turned on, as shown in Figure 6. However, as we see by comparing the upper part of Figure 4 with the calculated bistability between the oscillatory state and SSI in Figure 7, the calculated oscillatory state is not as robust to changes in flow rate as its experimental counterpart.

Owing to the reactions in group 4 of the mechanism, the low-pH SSII appears at input concentrations and flow rates close to those

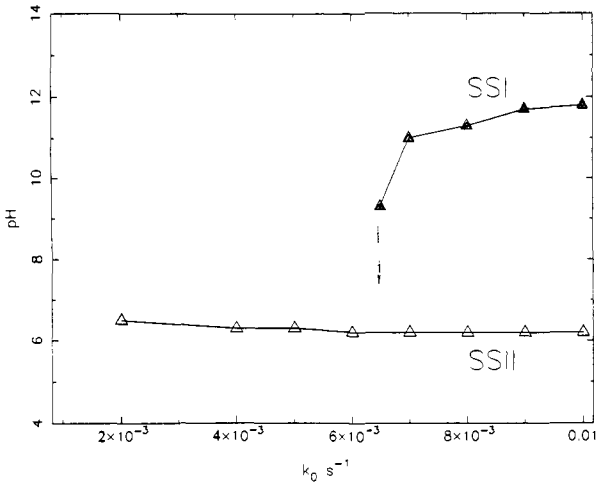


**Figure 8.** Calculated hysteresis between SSI and SSII: $[NaOH]_0 = 5.0 \times 10^{-3}$ M. Other conditions are the same as in Figure 5.

of the experiments. Figure 8 depicts the calculated SSI–SSII hysteresis, which is qualitatively similar to the lower part of Figure 4. However the search for bistability between the oscillatory state and SSII has proved unsuccessful to date. A complete phase diagram resembling Figure 4 has not been constructed because of the prohibitive amount of computing time that would be required for such a large system.

## Discussion

The proposed mechanism for the oscillatory $H_2O_2$–KSCN–$CuSO_4$ system, (M1)–(M30), has shown great success in simulating the observed oscillations in both batch and flow conditions. Despite the large number of steps and the difficulty of fitting 80% of the rate constants, the calculated results account well for most of the major dynamical features, including the period, magnitude, and the shape of the oscillation, as well as the multistable behavior.

Not surprisingly, some significant discrepancies remain between the results of our simulations and the experiments. For the batch behavior, only the effects of varying $[OH^-]_0$ are accurately reproduced by the simulations: at higher $[OH^-]_0$ the total number of oscillations increases while the period remains constant. When the other initial concentrations are varied, the effects are smaller than or even occasionally in the direction opposite to those of the experiments. The lower pH of the calculated SSII is 5.5, about one unit above that in the actual chemical system. As noted in the previous section, the range in $k_0$ of bistability between SSI and oscillation is much smaller than found experimentally, and we have been unable to reproduce the bistability between SSII and the oscillatory state.

One possible origin of these deficiencies is that the feedback scheme in the oscillation core is too simple, insufficient to maintain the oscillation at higher flow rates. Adding more reactions and more intermediates may help to increase the nonlinearity. However, without any evidence as to what species should be introduced, we hesitate to complicate further a mechanism that already contains 26 independent species. Other potential sources of discrepancy are the oversimplification of complex and protonation equilibria and inadequacies in our fitting of the unknown rate constants, perhaps as a result of cross correlations among them.

We emphasize that in a mechanism of this complexity the choice of intermediates, upon which the feedback loops are built, is not unique unless those intermediates have been experimentally verified or are well-known in the subsystems. What really matters, if not enough is known, is the overall structure of and competition between the feedback pathways. To illustrate this point, we give two examples of alternative oscillatory feedback networks that use completely different sets of intermediates but follow the same pattern in the positive and negative feedbacks. Both alternatives show batch and CSTR oscillations under the same conditions as the proposed mechanism.

1. Autocatalysis in SCN•:

$$SCN^\bullet + HOSCN \leftrightarrow HO(SCN)_2^\bullet \qquad k_{23}, k_{24} \qquad (23, 24)$$

$$HO(SCN)_2^\bullet + Cu^+\{SCN^-\}_n \rightarrow 2SCN^\bullet + Cu^{2+} + OH^- (+nSCN^-) \qquad k_{25} \quad (25)$$

$$SCN^\bullet + HO_2^\bullet \rightarrow HOOSCN \qquad k_{26} \qquad (26)$$

$$HOOSCN + HOSCN\ [+2OH^-] \rightarrow HSO_3^- + HOCN + SCN^- + H_2O \qquad k_{27} \quad (27)$$

$$2SCN^\bullet + OH^- \rightarrow HOSCN + SCN^- \qquad k_{28} \qquad (28)$$

Equations 23–25 accomplish the autocatalysis in the same manner as (M18)–(M20). Step 26 plays the same role as (M21), suppressing the autocatalysis, while (27) corresponds to (M22). Since both HOSCN and $Cu^+\{SCN^-\}_n$ are consumed during the autocatalysis, controlling the timing of the accumulation of either will yield the desired phase shift. Equation 28 is included for completeness. This alternative worked almost as well as our preferred mechanism in generating both batch and flow oscillations. No detailed studies of bistability in the CSTR were performed.

This scheme was rejected for several reasons: the radical–molecule adduct $HO(SCN)_2^\bullet$ seemed less plausible than the other postulated intermediates; oscillations ceased when a reaction between SCN• and $Cu^+\{SCN^-\}_n$ with a reasonable rate constant was included. Another serious drawback involves eq 26, which is crucial for the negative feedback chain. Pulse radiolysis experiments[23] show that the reaction should have a rate constant of $1.6 \times 10^9$ $M^{-1}$ $s^{-1}$, which is about 5 orders of magnitude higher than the maximum value that produces oscillation, and the products should be $SCN^-$ and $O_2$ instead of an adduct, HOOSCN.

2. Autocatalysis in $S_2O_4^{2-}$:

$$S_2O_4^{2-} + 2Cu^+\{SCN^-\}_n \rightarrow 2SO_2^{2-} + 2Cu^{2+}\{+nSCN^-\} \qquad k_{29} \quad (29)$$

$$SO_2^{2-} + {}^-OOS(O)CN \rightarrow S_2O_4^{2-} + {}^-OCN \qquad k_{30} \quad (30)$$

$$S_2O_4^{2-} + 2H_2O_2 \rightarrow S_2O_6^{2-} + 2H_2O \qquad k_{31} \quad (31)$$

$$S_2O_6^{2-} + 2Cu^+\{SCN^-\}_n \rightarrow 2SO_3^{2-} + 2Cu^{2+}\{+nSCN^-\} \qquad k_{32} \quad (32)$$

Again, the first two reactions give rise to autocatalysis in either $S_2O_4^{2-}$ or $SO_2^{2-}$, depending on how one sums the equations. The negative feedback and the phase shift, constituted by eq 31 and 32, have nearly the same pattern as the two previous examples. A significant difference is that in eq 31 $S_2O_4^{2-}$ is consumed by a reagent, which is always in large excess and monotonically decreasing, instead of by an autocatalytically produced intermediate. This fact causes the shape and the period of the calculated oscillations to be quite different from those in Figure 5. The period is much longer, and no more than four cycles are obtained before the oscillations die out.

Dithionite and dithionate ions are used extensively in the textile industry and in environmental research as powerful reductants. No examples have appeared in the literature in which they are reduced by a metal ion. The plausibility of eq 29 and 32 is therefore questionable. In addition, the potential for $Cu^{2+}/Cu^+$ in the presence of any plausible counterion should be much higher than that for $S_2O_4^{2-}/SO_2^{2-}$. A stopped-flow study by Creutz and Sutin[24] suggests that the reaction of hydrogen peroxide with dithionite is considerably more complex than implied by eq 31.

Of course, the above examples do not constitute all possible alternative mechanisms that can give rise to oscillations. Specifying the number of alternatives is as vain a goal as proving the validity of a single mechanism. By carrying out calculations on

(23) Adams, G. E.; Boag, J. C.; Michael, B. D. *Pulse Radiolysis*; Ebert, M., Keene, J. P., Swallow, A. J., Baxendale, J. H., Eds.; Academic Press: London, 1965; p 122.

(24) Creutz, C.; Sutin, N. *Inorg. Chem.* **1974**, *13*, 2041.

alternative mechanisms, one can gain deeper insights into how to construct better oscillatory mechanisms. The negative feedback scheme suggested in this work is only one of many possible patterns that are sufficient to generate oscillation when coupled to a similar positive feedback loop. Other types will be discussed elsewhere.

The proposed mechanism gives good agreement with the major observations on the rich dynamics of this exceedingly complex system. The remaining discrepancies with the experiments clearly call for further refinement or revision. Though the intermediates suggested must still be considered hypothetical, the calculations presented here suggest new approaches to the extremely difficult problem of mechanistic oxysulfur chemistry.

**Acknowledgment.** This work was supported by Grant CHE-8800169 from the National Science Foundation and by a U. S.-Hungarian cooperative grant from the NSF (INT-8613532) and the Hungarian Academy of Sciences.

**Registry No.** $H_2O_2$, 7722-84-1; $SCN^-$, 302-04-5; Cu, 7440-50-8.

# Conformational Analysis via NMR Isotope Shifts. Side-Chain Equilibria in *N*-Alkylpiperidines

**David A. Forsyth* and Vichukorn Prapansiri**

*Contribution from the Department of Chemistry, Northeastern University, Boston, Massachusetts 02115.* *Received October 5, 1988*

**Abstract:** Conformational equilibria involving the *N*-alkyl side chain of *N*-alkylpiperidines were detected via NMR isotope shifts. Introduction of a single deuterium at C1′ of the side chain causes a gauche ⇄ gauche equilibrium to be nondegenerate and observable by the separation of signals for C2 and C6 in $^{13}C$ NMR spectra at low temperature. The separation is temperature dependent, as expected for an equilibrium isotope effect. Actual $K_{iso}$ and $\Delta G°_{iso}$ for the isotopically perturbed equilibrium cannot be directly calculated by the application of Saunders' equation because the equilibration process is too rapid to obtain the maximum chemical shift difference between C2 and C6 at the slow exchange limit. Nonetheless, some useful estimates of these values can be made. The observations can be accounted for by the presence of both gauche and anti conformers in the equilibrium. MM2 calculations using Allinger's parameters for amines also support the conclusion that both gauche and anti conformers are present, with the proportion of gauche conformers declining in the sequence *N*-ethylpiperidine > *N*-propylpiperidine, *N*-butylpiperidine > *N*-benzylpiperidine.

Isotope effects on NMR chemical shifts can be used to differentiate equilibrating systems from static structures.[1] The technique is particularly well suited to detect degenerate equilibria, which have low energy barriers and are thus too rapid to be accessible by other NMR techniques. Bushweller et al. have demonstrated that some conformational equilibria occurring via C–N bond rotations in amines occur too rapidly to be detectable by ordinary dynamic NMR techniques.[2] For example, even at the temperature of 99 K where nitrogen inversion and one C–N bond rotation process were slow on the NMR time scale, it was still not possible to determine with certainty whether the major conformer of diethylmethylamine actually had $C_s$ symmetry or simply time-averaged symmetry due to very rapid C–N bond rotations.[2] In this paper we explore the application of the isotopic perturbation method to conformational analysis of acyclic alkyl chains of tertiary amines, with the specific example of *N*-alkylpiperidines. It has recently been reported that substantial conformational equilibrium isotope effects (CEIE)[3] are associated with deuteriation adjacent to the nitrogen in cyclic amines.[4-6] If this type of effect accompanies deuteriation of acyclic alkyl groups, it could be used to advantage in conformational analysis.

**Scheme I**

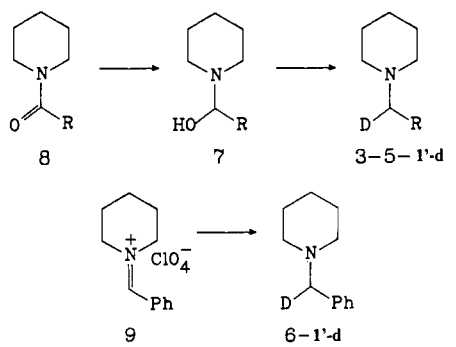


*N*-(*n*-Alkyl)piperidines can be assumed to have gauche **1** and/or anti **2** conformations, defined by the alignment of alkyl substituents relative to the nitrogen lone pair. In the case of the gauche conformation, there would be two isoenergetic enantiomeric structures, **1a** and **1b**. Interconversion among these three possible

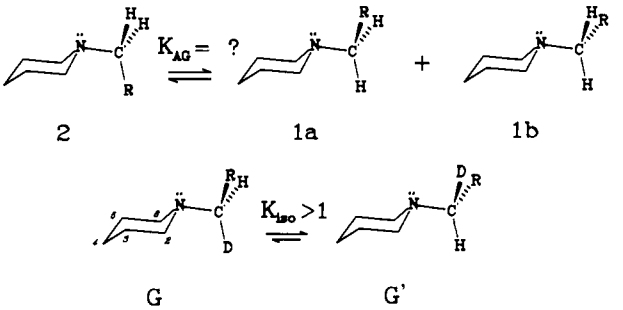


(1) (a) Saunders, M.; Kates, M. R. *J. Am. Chem. Soc.* **1977**, *99*, 8071. (b) Saunders, M.; Kates, M. R.; Wiberg, K. B.; Pratt, W. *J. Am. Chem. Soc.* **1977**, *99*, 8072. (c) For a recent review, see: Siehl, H. U. *Adv. Phys. Org. Chem.* **1987**, *23*, 63.

(2) Bushweller, C. H.; Fleischmann, S. H.; Grady, G. L.; McGoff, P.; Rithner, C. D.; Whalon, M. R.; Brennan, J. G.; Marcantonio, R. P.; Domingue, R. P. *J. Am. Chem. Soc.* **1982**, *104*, 6224.

(3) Baldry, K. W.; Robinson, M. J. T. *Tetrahedron* **1977**, *33*, 1663.

(4) Anet, F. A. L.; Kopelevich, M. *J. Chem. Soc., Chem. Commun.* **1987**, 595.

(5) Forsyth, D. A.; Hanley, J. A. *J. Am. Chem. Soc.* **1987**, *109*, 7930.

(6) Forsyth, D. A.; Prapansiri, V. *Tetrahedron Lett.* **1988**, *29*, 3551.

0002-7863/89/1511-4548$01.50/0 